

dithiothreitol (DTT), 10 mM adenosine diphosphate (ADP), and 10% glycerol. Crystallization was initiated by the addition of microseeds, prepared from substrate crystals, after 14 to 20 hours. Plate-like crystals grew in about 10 days. The crystals were harvested in solutions containing 20% (w/v) PEG 4000, 0.3 M ammonium acetate, 25 mM Na-Hepes (pH 7.5), 50 mM DTT, 10 mM ADP and 10% glycerol. For cryoprotection, the crystals were transferred to solutions containing increasing glycerol (15, 20, and 25%) for about 1 min each and flash-cooled in liquid propane. Initial data for a rosuvastatin complex structure to a resolution of 2.4 Å were collected at beamline 5.0.2 of the Advanced Light Source (ALS) synchrotron, which is supported by the Director, Office of Science, Office of Basic Energy Sciences, Materials Sciences Division of the U.S. Department of Energy under Contract No. DE-AC03-76SF00098 at Lawrence Berkeley National Laboratory. Data for the other inhibitor complexes and higher resolution data for the rosuvastatin complex were collected at beamline F1 at the Cornell High Energy Synchrotron Source (CHESS), which is supported by the National Science Foundation under award DMR-9311772, using the Macromolecular Diffraction at CHESS (MacCHESS) facility, which is supported by award RR-01646 from the National Institutes of Health. Data reduction and processing were carried out with the HKL package (75). Because the low-resolution data for the rosuvastatin complex crystal was incomplete for the data collected at CHESS, the reduced data were merged with the reduced data collected at ALS during scaling. All crystals have the symmetry of space group P2<sub>1</sub> and contain four HMGR monomers in each asymmetric unit, although two different crystal forms were observed (Table 1). The protein portion of the structure of human HMGR in complex with HMG, CoA, and NADP<sup>+</sup> [Protein Data Bank (PDB) code 1dqa] was used as the starting model for the refinement. Initially, the inhibitor molecules were placed into F<sub>o</sub>-F<sub>c</sub> electron-density maps. Subsequently, their positions were modified by consulting  $\sigma_A$  weighted 2F<sub>o</sub>-F<sub>c</sub> maps (16) and simulated-annealing omit maps (17). The models were built using the program O (18) and refined with CNS (19). Bulk solvent, overall anisotropic B-factor scaling, and noncrystallographic symmetry restraints were applied throughout the refinement process. For each of the six HMGR-statin complexes, the electron-density maps were excellent for all four statin molecules bound to the four crystallographically independent monomers. Additionally, poor electron density was located close to residues Y479 and F629 (20) and was interpreted as ADP. The positions of the ADP molecules resemble the positions of the adenosine moieties of the substrates CoA or NADPH. ADP was bound only to some of the CoA or NADPH binding sites and the number of ADP molecules is different for the six structures.

11. C. M. Lawrence, V. W. Rodwell, C. V. Stauffer, *Science* **268**, 1758 (1995).
12. L. Taberner, D. A. Bochar, V. W. Rodwell, C. V. Stauffer, *Proc. Natl. Acad. Sci. U.S.A.* **96**, 7167 (1999).
13. All calculations on accessible or buried surface areas for the statins or the protein, as well as distance information between specific groups, represent averages for the four crystallographically independent statin molecules observed in each complex structure. The surface accessible areas for the unbound statins, the bound statins, and the buried surface areas upon statin binding to HMGR, respectively, are as follows: compactin 670 Å<sup>2</sup>, 100 Å<sup>2</sup>, 880 Å<sup>2</sup>; simvastatin 670 Å<sup>2</sup>, 110 Å<sup>2</sup>, 880 Å<sup>2</sup>; fluvastatin 660 Å<sup>2</sup>, 80 Å<sup>2</sup>, 870 Å<sup>2</sup>; cerivastatin 720 Å<sup>2</sup>, 100 Å<sup>2</sup>, 880 Å<sup>2</sup>; atorvastatin 840 Å<sup>2</sup>, 150 Å<sup>2</sup>, 1060 Å<sup>2</sup>; and rosuvastatin 710 Å<sup>2</sup>, 130 Å<sup>2</sup>, 880 Å<sup>2</sup>.
14. M. S. Brown, J. R. Faust, J. L. Goldstein, *J. Biol. Chem.* **253**, 1121 (1978).
15. Z. Otwinowski, W. Minor, *Methods Enzymol.* **276**, 306 (1997).
16. A. Hodel, S.-H. Kim, A. T. Brünger, *Acta Crystallogr. A* **48**, 851 (1992).
17. R. J. Read, *Acta Crystallogr. A* **1986**, 140 (1986).

18. T. A. Jones, J. Y. Zou, S. W. Cowan, M. Kjeldgaard, *Acta Crystallogr. A* **47**, 110 (1991).
19. A. T. Brünger *et al.*, *Acta Crystallogr. D* **54**, 905 (1998).
20. Single-letter abbreviations for the amino acid residues are as follows: A, Ala; C, Cys; D, Asp; E, Glu; F, Phe; G, Gly; H, His; I, Ile; K, Lys; L, Leu; M, Met; N, Asn; P, Pro; Q, Gln; R, Arg; S, Ser; T, Thr; V, Val; W, Trp; and Y, Tyr.
21. G. A. Holdgate *et al.*, in preparation.
22. R. M. Esmouf, *Acta Crystallogr. D* **55**, 938 (1999).
23. L. Esser, personal communication.

24. Persistence of Vision Ray Tracer v.3.02. Copyright 1997, POV-Team. www.povray.org
25. We thank AstraZeneca for providing simvastatin, fluvastatin, cerivastatin, atorvastatin, and rosuvastatin and for stimulating discussions; S. Jeong for converting compactin to the active sodium salt form; the personnel at ALS beamline 5-1 and CHESS beamline F1 for their assistance in data collection; and C. A. Brautigam for critical reading of the manuscript. The coordinates are available from the PDB (accession numbers are indicated in Table 1).

26 January 2001; accepted 3 April 2001

## Control of a Genetic Regulatory Network by a Selector Gene

Kirsten A. Guss,\* Craig E. Nelson,\* Angela Hudson, Mary Ellen Kraus, Sean B. Carroll†

The formation of many complex structures is controlled by a special class of transcription factors encoded by selector genes. It is shown that SCALLOPED, the DNA binding component of the selector protein complex for the *Drosophila* wing field, binds to and directly regulates the cis-regulatory elements of many individual target genes within the genetic regulatory network controlling wing development. Furthermore, combinations of binding sites for SCALLOPED and transcriptional effectors of signaling pathways are necessary and sufficient to specify wing-specific responses to different signaling pathways. The obligate integration of selector and signaling protein inputs on cis-regulatory DNA may be a general mechanism by which selector proteins control extensive genetic regulatory networks during development.

The concept of the morphogenetic field, a discrete set of cells in the embryo that gives rise to a particular structure, has held great importance in experimental embryology (1). The discovery of genes whose products control the formation and identity of various fields, dubbed "selector genes" (2), has enabled the recognition and redefinition of fields as discrete territories of selector gene activity (3). Although the term has been used somewhat liberally, two kinds of selector genes have been of central interest to understanding the development of embryonic fields. These include the *Hox* genes, whose products differentiate the identity of homologous fields, and field-specific selector genes such as *eyeless* (4), *Distal-less* (5), and *vestigial-scalloped* (*vg-sd*) (6–8), whose products have the unique property of directing the formation of entire complex structures. The mechanisms by which field-specific selector proteins direct the development of these structures are not well understood. In principle, selector proteins could directly regulate the expression of only a few genes, thus exerting much of their effect indirectly, or they may regulate the tran-

scription of many genes distributed throughout genetic regulatory networks.

In the *Drosophila* wing imaginal disc, the VG-SD selector protein complex regulates wing formation and identity (7, 8). SD is a TEA-domain protein (9) that binds to DNA in a sequence-specific manner (7), whereas VG, a novel nuclear protein (10), functions as a trans-activator (11). To determine whether direct regulation by SD is widely required for gene expression in the wing field, we analyzed the regulation of several genes that represent different nodes in the wing genetic regulatory network and that control the development of different wing pattern elements (Fig. 1A). We focused in particular on genes for which cis-regulatory elements that control expression in the wing imaginal disc have been isolated, including *cut* (12), *spalt* (*sal*) (13), and *vg* (6).

We first tested whether *sd* gene function was required for the expression of various genes in the wing field. We generated mitotic clones of cells homozygous for a strong hypomorphic allele of *sd* and assessed the expression of gene products or reporter genes within these clones (14). Reduction of *sd* function reduced or eliminated the expression of the CUT (Fig. 1, B and F) and WINGLESS (WG) (Fig. 1, C and G) proteins and of reporter genes under the control of the *sal* 10.2-kb (Fig. 1, D and H) and the *vg* quadrant (Fig. 1, E and I) enhancers.

Howard Hughes Medical Institute and Laboratory of Molecular Biology, University of Wisconsin, Madison, WI 53706, USA.

\*These authors contributed equally to this work.

†To whom correspondence should be addressed. E-mail: sbcarroll@facstaff.wisc.edu

REPORTS

demonstrating a cell-autonomous requirement for selector gene function for the expression of these genes in the wing field.

These results, however, do not distinguish between the direct and indirect regulation of target gene expression by VG-SD. To differentiate between these possibilities, we tested whether the DNA binding domain of SD could bind to specific sequences in *cut*, *sal*, and *vg* wing-specific cis-regulatory elements (15). Us-

ing DNase I footprinting, we identified SD-binding sites in all of the elements assayed (Fig. 2A) (16). Thus, SD may control the expression of these genes by binding to their cis-regulatory elements.

To determine whether SD binding to these sites was necessary for the function of these cis-regulatory elements in vivo, we mutated specific SD-binding sites within each of the elements such that they reduced or abolished SD binding in gel mobility-shift assays (Fig. 2, B and C) (17). The mutation of tandem SD-binding sites in the *cut* and *sal* elements resulted in complete loss of reporter gene expression in vivo (Fig. 2, G and H). Similarly, mutation of the four single SD-binding sites identified in the *vg* quadrant enhancer eliminated or dramatically reduced reporter gene expression (Fig. 2I). These results show that SD binds to and directly regulates the expression of four genes—*cut*, *sal*, *vg*, and DSRF (7)—in the wing genetic regulatory network. This molecular analysis and the genetic requirement for SD function for the expression of other genes (18) suggest a widespread requirement for direct VG-SD regulation of genes expressed in the wing field.

Each of the SD targets we analyzed is activated in only a portion of the wing field, in patterns controlled by specific signaling pathways. For instance, *cut* is a target of Notch

signaling along the dorsoventral boundary (19–21), and the *sal* and *vg* quadrant enhancers are targets of Dpp signaling along the anteroposterior axis (22–26). Binding sites for the transcriptional effectors of the Notch- and Dpp-signaling pathways, Suppressor of Hairless [SU(H)], and Mothers Against Dpp (MAD), and Medea (MED), respectively (24, 27, 28), have been shown to be necessary for the activity of a number of wing-specific cis-regulatory elements (6, 24, 29) and occur in these elements (Fig. 2A). This observation, coupled with our data demonstrating a direct requirement for SD binding, suggests that gene expression in the wing field requires two discrete inputs on the cis-regulatory DNA: one from the selector proteins that define the field, and one from the signaling pathway that patterns the field.

These findings also raised the possibility that the combination of selector and signal inputs may be sufficient to drive field-specific, patterned gene expression. To test this, we built a number of synthetic regulatory elements comprised of combinations of binding sites for SD with those for SU(H) or MAD/MED (30). We compared the activity of these elements with those composed of tandem arrays of just selector- or signal effector-binding sites, or combinations of different signal effector sites. Each of the binding sites used

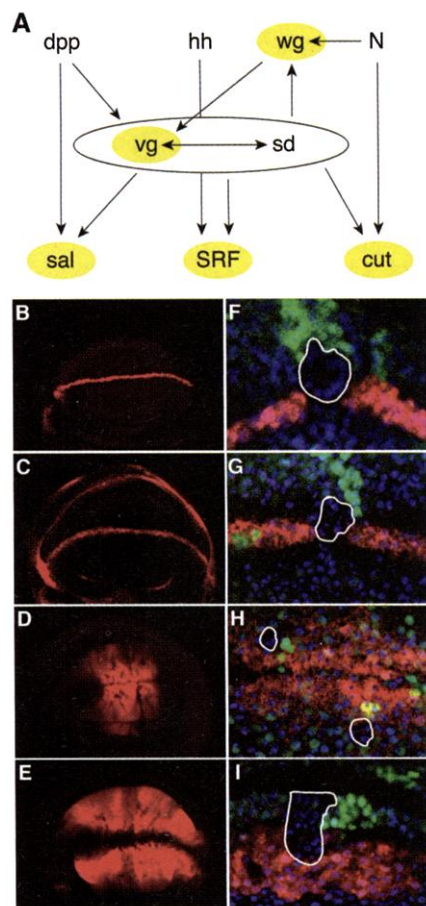


**Fig. 1.** SD function is required for wing-specific target gene expression. (A) A simplified portion of a genetic regulatory network in the wing disc, including those signaling pathways and target genes analyzed here (highlighted in yellow). (B to I) Gene expression in the wing pouch is dependent upon SD activity. Protein or reporter gene expression in late third larval instar wing imaginal discs is shown (red in B to E, magenta in F to I). Mitotic clones homozygous for the hypomorphic *sd<sup>58</sup>* allele are marked by the absence of the Myc epitope tag (green in F to I) and are circled, and cells are marked by the nuclear dye TOPRO (blue in F to I). (B and F) CUT protein expression along the D-V boundary. (C and G) WG protein expression along the D-V boundary. (D and H)  $\beta$ -Galactosidase expression driven in a broad domain straddling the A-P boundary by the *sal* 10.2-kb element (13), and (E and I) by the *vgQ* enhancer throughout the wing blade except along the D-V boundary (6). The expression of each candidate target gene is eliminated or reduced by the reduction of SD function.

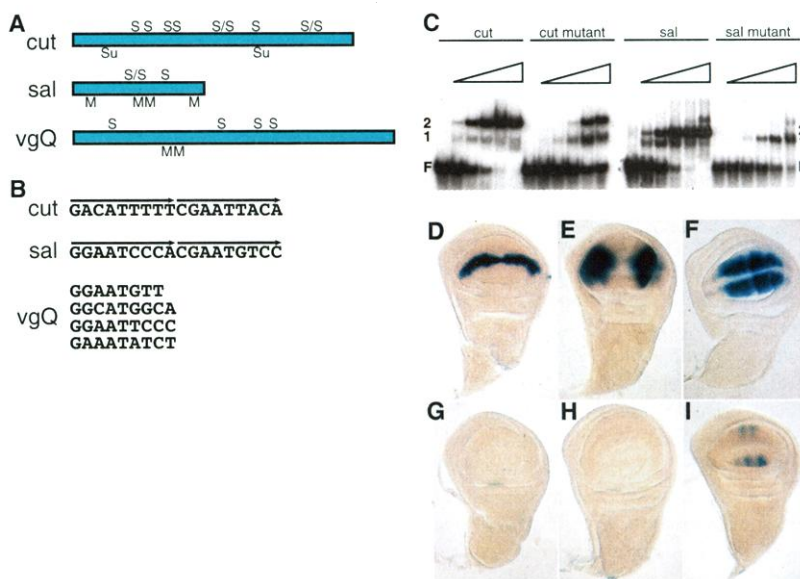


**Fig. 2.** SD protein binds to and directly regulates the expression of multiple wing-specific cis-regulatory elements in vivo. (A) The topology of sites that bind SD (S; tandem sites denoted S/S), SU(H) (Su), and MAD (M) in the *cut*, *sal*, and *vg* cis-regulatory elements. (B) The sequences of SD-binding sites that have been shown to be required for the activity of wing-specific cis-regulatory elements. Tandem sites have arrows over them. (C) Gel mobility-shift experiments with wild-type and mutated double-stranded oligonucleotide probes spanning tandem SD-binding sites in the *cut* 0.7-kb and *sal* 328-base pair (bp) elements. Increasing amounts of SD TEA domain utilized for each probe were, from left to right, 0, 0.1, 0.3, 1, 3, and 10 ng/25  $\mu$ l. Labels: F, free probe; 1, complex with one SD TEA domain bound; 2, complex with two molecules bound. (D to I)  $\beta$ -Galactosidase expression driven by the (D) *cut* 0.7-kb, (E) *sal* 328-bp, and (F) *vgQ* enhancers, respectively, in late third larval instar wing imaginal discs. (G) Expression driven by the *cut* 0.7-kb enhancer in which the tandem SD-binding sites have been altered. (H) The tandem SD sites in the *sal* 328-bp element shown in (H) are required for wing expression. (I) Expression driven by the *vgQ* enhancer, in which four single SD-binding sites have been mutated, is significantly reduced or eliminated.

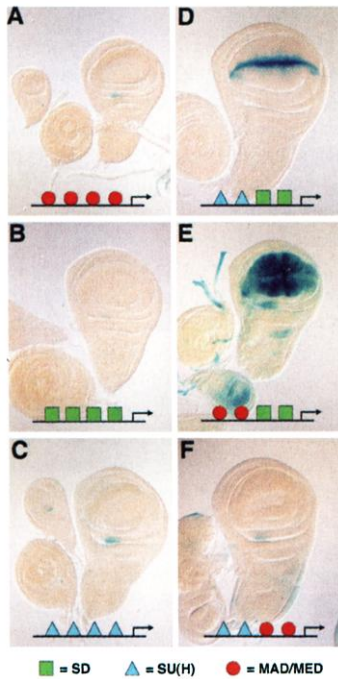
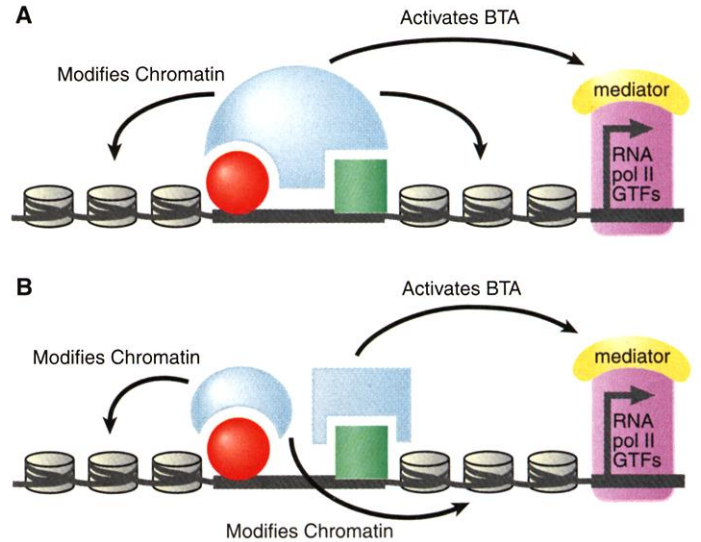


**Fig. 3.** Combinatorial regulation of gene expression in the wing field. Reporter gene expression driven by synthetic regulatory elements in *Drosophila* late third larval instar wing imaginal discs. Synthetic elements were composed of the following: (A) two MAD- and two MEDEA-binding sites, (B) four SD-binding sites, (C) four SU(H)-binding sites, (D) two SU(H)-binding sites and two SD-binding sites, (E) a MAD- and a MEDEA-binding site and two SD-binding sites, (F) a MAD- and MEDEA-binding site and two SU(H)-binding sites. MAD- and MEDEA-binding sites are represented by red circles, SU(H)-binding sites by blue triangles, and SD-binding sites by green squares.

in these constructs was selected from sequences found in native *Drosophila* cis-regulatory elements that have been demonstrated to function in vivo (6, 7, 24).

Elements containing only single classes of binding sites for the selector or signal effectors were unable to drive reporter gene expression in the wing (Fig. 3, A to C). In contrast, the synthetic elements in which binding sites for both selector and signal effector were combined drove field-specific expression restricted to the wing and haltere discs in patterns predicted by the specific signaling inputs to each element. That is, the [SD]<sub>2</sub> [SU(H)]<sub>2</sub> element drove wing-specific expression along the dorsoventral margin (Fig. 3D), consistent with Notch activation along this boundary (19, 20, 31), and the [SD]<sub>2</sub> [MAD/MED] element drove expression in a broad domain oriented with respect to the anteroposterior axis of the disc (Fig. 3E), consistent with Dpp-signaling activity along this boundary (32, 33). These patterns of expression are similar to those of the native *cut* and *vg* quadrant cis-regulatory elements that also respond to Notch- and Dpp-signaling inputs, respectively. However, regulatory elements con-

**Fig. 4.** Models for the field-specific control of transcription by selector proteins and signal effectors. Our results suggest that only when binding sites for both classes of transcription factors are occupied is a functional activation complex assembled and the basal transcriptional apparatus (BTA) enabled. (A) The two transcription factors could bind to different faces of the same coactivator (in blue, e.g., CBP), which could mediate chromatin remodeling via histone acetyltransferase and could mediate interactions with the BTA. (B) Alternatively, transcriptional effectors of signaling pathways and selector proteins may recruit different coactivators (in blue) that perform these functions independently.



taining a combination of SU(H) and MAD/MED sites were not active in vivo (Fig. 3F), demonstrating that combinatorial input in the absence of selector input is not sufficient to drive gene expression. These results suggest that the VG-SD complex provides a qualitatively distinct function required to generate a wing-specific response to signaling pathways.

There are several potential mechanisms whereby selector proteins and signaling effectors might operate in a combinatorial manner to regulate transcription. One mechanism is through cooperative interactions that increase the occupancy of transcription factor-binding sites on the DNA. Such a scenario appears unlikely in this case, because it would require that each selector protein be able to interact directly with many different signaling pathway transcriptional effectors. Furthermore, cooperative filling of binding sites alone is insufficient to explain selector-signal synergy, because SD alone binds cooperatively to DNA [Fig. 2C and (7)], and yet the presence of multiple SD-binding sites alone is insufficient to generate transcriptional activation.

A second, more likely mechanism underlying selector-signal synergy is the formation of complexes between the two classes of transcription factors and required transcriptional co-activators. Coactivators facilitate transcription by relieving repression by chromatin and/or by mediating interactions with the basal transcriptional machinery (34). We suggest that gene activation by selector proteins and signaling pathways may require both of these activities, and these proteins may form complexes with coactivators on the cis-regulatory DNA (Fig. 4). These complexes could include coactivators such as the multifunctional protein CBP, which

has been shown to interact directly with three signaling pathway transcriptional effectors, MAD, CI, and dTCF (35), and also appears to interact with SD (36). Alternatively, synergy between SD and signaling pathway transcriptional effectors could be mediated by different coactivators, with independent functions (Fig. 4B). The obligate requirement for combined inputs from selector genes and signaling pathways, seen here in the wing, may be a general mechanism whereby a universally deployed set of signals can elicit field, tissue, and cell type-specific genetic responses (37).

**References and Notes**

1. S. F. Gilbert, J. M. Opitz, R. A. Raff, *Dev. Biol.* **173**, 357 (1996).
2. A. Garcia-Bellido, *Ciba Found. Symp.* **29**, 161 (1975).
3. R. S. Mann, G. Morata, *Annu. Rev. Cell Dev. Biol.* **16**, 243 (2000).
4. G. Halder, P. Callaerts, W. Gehring, *Science* **267**, 1788 (1995).
5. S. Cohen, M. Bronner, F. Kuttner, G. Jurgens, H. Jackle, *Nature* **338**, 432 (1989).
6. J. Kim, A. Sebring, J. Esch, M. Kraus, K. Vorwerk, J. Magee, S. Carroll, *Nature* **382**, 133 (1996).
7. G. Halder, P. Polaczyk, M. E. Kraus, A. Hudson, J. Kim, A. Laughon, S. B. Carroll, *Genes Dev.* **12**, 3900 (1998).
8. A. Simmonds, X. Liu, K. Soanes, H. Krause, K. Irvine, J. Bell, *Genes Dev.* **12**, 3815 (1998).
9. P. Jacquemin, I. Davidson, *Trends Cardiovasc. Med.* **7**, 192 (1997).
10. J. A. Williams, J. Bell, S. B. Carroll, *Genes Dev.* **5**, 2481 (1991).
11. P. Vaudin, R. Delanoue, I. Davidson, J. Silber, A. Zider, *Development* **126**, 4807 (1999).
12. J. Jack, D. Dorsett, Y. Delotto, S. Liu, *Development* **113**, 735 (1991).
13. R. Kuhnlein, G. Bronner, H. Taubert, R. Schuh, *Mech. Dev.* **66**, 107 (1997).
14. Flies of genotype *w<sup>sd<sup>5B</sup></sup>* P[ry<sup>+</sup>, *hs-neo*, *FRT*]18A/Y carrying the P element of interest on the second or third chromosome were mated to *w<sup>P[w<sup>+</sup>]; *hs-πM*]</sup>* 5A, 10D P[ry<sup>+</sup>; *hs-neo*, *FRT*]18A; *hsflp3MKRS/TM6B* females. Clones were induced in progeny 72 to 96 hours after egg laying by heat shock at 37°C for 1 to 2 hours. Larvae were aged an additional 48 hours, heat shocked for 2 hours at 37°C to induce MYC expression, and incubated at 25°C for 30 to 120 min

before fixation. Wandering third instar female larval imaginal discs were dissected, fixed, blocked, incubated with antibodies, washed and mounted as described in J. Kim *et al.*, *Cell* **82**, 795 (1995). Antibodies and the dilutions at which they were used were: rabbit antibody against  $\beta$ -galactosidase (Cappel or Molecular Probes; 1:500 or 1:1000); mouse antibody against MYC (provided by S. Blair; 1:4); rabbit antibody against MYC (Santa Cruz Biotechnology; 1:200); rabbit antibody against WG (provided by S. Cumberledge; 1:1000); mouse anti body against CUT (Developmental Studies Hybridoma Bank; 1:4). X-gal staining was performed as described [Y. Hiromi, W. J. Gehring, *Cell* **50**, 963 (1987)].

15. The *cut* 0.7-kb cis-regulatory element is the 0.7 kb at the 3' end of the *cut* gene wing margin enhancer (12), which drives reporter gene expression along the presumptive wing margin. The *sal* 328-bp enhancer is a subfragment of the *sal* 10.2-kb enhancer (13), that drives expression in a wing pouch-restricted, albeit altered, pattern. Reporter constructs were made by cloning polymerase chain reaction (PCR)-generated fragments of the *cut* gene wing margin or *sal* enhancers into the Hsp *lacZ*-CaSpeR plasmid [H. Nelson, A. Laughon, *Roux's Arch. Dev. Biol.* **202**, 341 (1993)]. The GenBank accession numbers for the *cut* 0.7-kb and *sal* 328-bp cis-regulatory elements are AF369916 and AF369917, respectively.

16. Generation of the SD TEA domain, DNase I footprinting, and electrophoretic mobility-shift assays were performed as described (7). Probes for footprinting were generated by end-filling subfragments of cis-regulatory elements with radioactively labeled nucleotides. Probes for shifts were annealed oligonucleotides that were radioactively labeled by kinase or end-filling with Klenow. Sequences protected by the SD TEA domain were aligned and analyzed using the PileUp program of GCG [Wisconsin Package Version 9.1, Genetics Computer Group (GCG), Madison, WI], with adjustments by hand.

17. Sequences of the upper strand of oligonucleotides used as probes for shifts and as PCR primers to mutate SD-binding sites (positions noted in parentheses) in the various cis-regulatory elements are listed in the 5' to 3' orientation. Altered bases are shown in lowercase in the mutant version, and the corresponding bases are underlined in the native sequence. At least three independent transgenic lines were analyzed for each set of SD sites mutated.

*sal* (126) wild type:  
5' TTAAGATGCTTCTTGAATCCCACGAATGTC-  
ATTGGATGG 3'

*sal* (126) mutant:  
5' TTAAGATGCTTCTctAATcagActAATgaggATTGG-  
ATGG 3'

*cut* (558) wild type:  
5' TTGTCAATGTAATTCGAAAATGTCGTGAG 3'

*cut* (558) mutant:  
5' TTGTCAATcTAATTctActAATtTCGTGAG 3'

*vgQ* 1 (87) wild type:  
5' GCGTTGACAAcATTCcAAACTCG 3'

*vgQ* 1 (87) mutant:  
5' GCGTTGACAtgAgctCttACTCG 3'

*vgQ* 2 (359) wild type:  
5' ATACGGGATGcCATGcCGCGTGC 3'

*vgQ* 2 (359) mutant:  
5' ATACGGGATctCATGagCGGTGC 3'

*vgQ* 3 (450) wild type:  
5' GAGCCGTGGAATTCcCATTAATG 3'

*vgQ* 3 (450) mutant:  
5' GAGCCGTctAATTagCATTAATG 3'

*vgQ* 4 (488) wild type:  
5' CTGCCAAAGATATTTCCTCTGCAG 3'

*vgQ* 4 (488) mutant:  
5' CTGCCAAActTATTTCTCTGCAG 3'

18. X. Liu, M. Grammont, K. D. Irvine, *Dev. Biol.* **228**, 287 (2000).

19. de J. Celis, A. Garcia-Bellido, S. Bray, *Development* **122**, 359 (1996).

20. C. Neumann, S. Cohen, *Development* **122**, 3477 (1996).

21. C. Micchelli, E. Rulifson, S. Blair, *Development* **124**, 1485 (1997).

22. J. de Celis, R. Barrio, F. Kafatos, *Nature* **381**, 421 (1996).

23. M. Zecca, K. Basler, G. Struhl, *Cell* **87**, 833 (1996).

24. J. Kim, K. Johnson, S. B. Carroll, A. Laughon, *Nature* **388**, 304 (1997).

25. C. J. Neumann, S. M. Cohen, *Development* **124**, 871 (1997).

26. K. Certel, A. Hudson, S. B. Carroll, W. A. Johnson, *Development* **127**, 3173 (2000).

27. A. M. Bailey, J. W. Posakony, *Genes Dev.* **9**, 2609 (1995).

28. J. B. Hudson, S. D. Podos, K. Keith, S. L. Simpson, E. L. Ferguson, *Development* **125**, 1407 (1998).

29. D. T. Nellesen, E. C. Lai, J. W. Posakony, *Dev. Biol.* **213**, 33 (1999).

30. Synthetic regulatory elements were constructed by ligating annealed oligonucleotide pairs encoding paired transcription factor-binding sites into the Eco RI and Asp<sup>718</sup> sites of Hsp *lacZ*-CaSpeR. Each construct consisted of an "A" and a "B" set of annealed oligonucleotides joined with a Bgl II site. The sequences of the top strand for each of the oligonucleotide pairs are as follows, listed in the 5' to 3' orientation: [SD]<sub>2</sub>-A, aattcccaAACTATGcCAGGAATT-Taaa; [SD]<sub>2</sub>-B, gatctccaAACTATGcCAGGAATT-Taaagaattcg; [SU(H)]<sub>2</sub>-A, aattGTTCTCACGgattcgaagGTTCTCACG; [SU(H)]<sub>2</sub>-B, gatctGTTCTCACGgattcgaagGTTCTCACGgattcg; [MADMED]-A, aattGC-CGTGCGgattcgaagGTTGCGCGGCa; [MADMED]-B, gatctGCGGTGCGgattcgaagGTTGCGCGGCaattcg. The transcription factor-binding sites within each oligonucleotide are capitalized; linker sequences are in lower case. In each of the signal and selector constructs the annealed 5' signal oligonucleotide pair (A) was ligated to the 3' selector oligonucleotide pair (B). In signal alone or selector alone constructs, the 5' and 3' pairs of the appropriate sites were ligated to one another. Wing disc-specific reporter expression was observed in 6 out of 8 lines for [SU(H)]<sub>2</sub> [SD]<sub>2</sub>; 3

out of 7 lines for [MADMED]<sub>2</sub> [SD]<sub>2</sub>; 1 out of 17 lines for [SU(H)]<sub>2</sub>; 1 out of 17 lines for [MADMED]<sub>2</sub>; and 1 out of 15 lines for [SD]<sub>2</sub>.

31. J. Williams, S. Paddock, K. Vorwerk, S. Carroll, *Nature* **368**, 299 (1994).

32. D. Nellen, R. Burke, G. Struhl, K. Basler, *Cell* **85**, 357 (1996).

33. T. Lecuit, W. Brook, M. Ng, M. Calleja, H. Sun, S. Cohen, *Nature* **381**, 387 (1996).

34. R. D. Kornberg, *Trends Cell Biol.* **9**, M46 (1999).

35. H. R. Goodman, S. Smolik, *Genes Dev.* **14**, 1553 (2000).

36. SD binds to discrete domains of CBP in vitro but does not interact with MAD or SU(H) (C. E. Nelson, S. B. Carroll, unpublished observations).

37. N. C. Grieder, T. Marty, H.-D. Ryoo, R. S. Mann, M. Affolter, *EMBO J.* **16**, 7402 (1997).

38. We thank D. Nellen for identifying and providing the *sal* 328-bp element and transgenic flies; S. Blair, K. Irvine, R. Schuh, and J. Jack for providing fruit fly stocks; T. Stone and J. Posakony for SU(H) protein; A. Laughon for MAD protein and probes; D. Dorsett for *cut* sequence and DNA; V. Kassner, J. Selegue, and K. Vacarro for invaluable technical assistance; L. Olds for figure preparation; J. Carroll for manuscript preparation; M. Levine for helpful discussion; and A. Kopp, G. Panganiban, and T. Wittkopp for comments on the manuscript. J. Magee initiated the studies of SD site mutations in the *vg Q* enhancer, and J.-Y. Sgro and the Institute for Molecular Virology provided access to GCG. Supported by NIH postdoctoral fellowships to K.A.G. and M.E.K., and the Howard Hughes Medical Institute, of which S.B.C. is an Investigator.

14 December 2000; accepted 20 March 2001  
Published online 12 April 2001;  
10.1126/science.1058312  
Include this information when citing this paper.

## Physical Properties Determining Self-Organization of Motors and Microtubules

Thomas Surrey,\* François Nédélec,\* Stanislas Leibler,† Eric Karsenti‡

In eukaryotic cells, microtubules and their associated motor proteins can be organized into various large-scale patterns. Using a simplified experimental system combined with computer simulations, we examined how the concentrations and kinetic parameters of the motors contribute to their collective behavior. We observed self-organization of generic steady-state structures such as asters, vortices, and a network of interconnected poles. We identified parameter combinations that determine the generation of each of these structures. In general, this approach may become useful for correlating the morphogenetic phenomena taking place in a biological system with the biophysical characteristics of its constituents.

A central question in biology concerns the origin of complex macroscopic structures. Two fundamentally different mechanisms can account for the generation of large-scale structures from random mixtures of small molecules. One mechanism is self-assembly near thermo-

dynamic equilibrium (1, 2). A very different mechanism is self-organization in energy-dissipating systems. Although they do not reach thermodynamic equilibrium, these systems can reach steady states; kinetic parameters can influence or determine the final structures (3, 4). In eukaryotic cells, organization of the intracellular architecture is largely determined by the collective behavior of the ensemble of proteins that constitute the cytoskeleton (5, 6). A remarkable property of the cytoskeleton resides in the versatility of all patterns that can be produced. Indeed, similar sets of components are found to be organized into very different assem-

Cell Biology and Biophysics Program, European Molecular Biology Laboratory, 69117 Heidelberg, Germany.

\*These authors contributed equally to this work.

†Present address: Departments of Physics and Molecular Biology, Princeton University, Princeton, NJ 08544, USA.

‡To whom correspondence should be addressed. E-mail: karsenti@embl-heidelberg.de